Materials Transactions, Vol. 48, No. 5 (2007) pp. 1124 to 1130

EXPRESS REGULAR ARTICLE

Mechanical Properties and Phase Stability of Ti-Nb-Ta-Zr-O Alloys

Tadahiko Furuta[1], Shigeru Kuramoto[1], Junghwan Hwang[1], Kazuaki Nishino[1], Takashi Saito[1] and Mitsuo Niinomi[2]

[1]*Materials Department, Toyota Central Research & Development Laboratories Inc., Nagakute, Aichi 480-1192, Japan*
[2]*Department of Biomaterials Science, Institute for Materials Research, Tohoku University, Sendai 980-8577, Japan*

The effects of niobium and oxygen content on the mechanical properties, β phase stability and elastic deformation behavior of Ti-Nb-Ta-Zr-O alloys were investigated by employing tensile tests, microstructure observations and XRD analysis. The basic composition of the tested alloys used was Ti-36%Nb-2%Ta-3%Zr-0.3%O (mass%), with the other alloys having lower niobium content (from 32% to 36%) and higher oxygen content (0.5%). Orthorhombic α'' was observed in the specimens with lower niobium content. Work hardening and elastic deformation behavior in the specimens with lower niobium (33% to 34%) and higher oxygen (0.5%) contents are similar to those of the alloy with basic composition; these specimens showed little work hardening and non-linearity in the elastic range of tensile deformation. The phase configuration analysis of these specimen alloys does not show the presence of any peaks other than the β phase before and after cold working. The cold worked Ti-32%Nb-2%Ta-3%Zr-0.5%O has a Young's modulus of 55 GPa, a tensile strength of 1370 MPa and a tensile elongation of 12%. After heat treatment at 623 K for 600 s, the tensile strength of the alloy reaches 1500 MPa, with a Young's modulus of 58 GPa and a tensile elongation of 10%. [doi:10.2320/matertrans.48.1124]

(Received March 6, 2007; Accepted March 19, 2007; Published April 25, 2007)

Keywords: *β phase stability, titanium-niobium-tantalum-zirconium-oxygen, high tensile strength, low Young's modulus, work hardening behavior, aging treatment*

1. Introduction

Some metastable β Ti-Nb-Ta-Zr-O alloys have outstanding mechanical and physical properties, such as a low Young's modulus with high strength, a low thermal expansion and good hot and cold workability.[1–5] Ti-Nb-Ta-Zr-O alloys also have good bio-compatibility and corrosion-resistance.[6–10] Due to these experimental results, these alloys have gotten a lot of attention recently as metallic biomaterials for use in artificial bones or implants,[11,12] which require low Young's modulus (10–30 GPa) and high strength when subjected to cycle loading under complicated conditions.[13]

Phase stability, which is strongly associated with the mechanical and physical properties of the alloys, depends on the contents of the Group Va elements, niobium and tantalum, and oxygen. Recently, many researchers have actively investigated the effect of the niobium, tantalum, zirconium and oxygen content on the β phase stability and mechanical properties in the Ti-Nb-Ta-Zr-O system. For instance, Sakaguchi *et al.*[14] showed that Ti-30Nb-10Ta-5Zr (mass%) alloy, which is a simplified version of the Ti-29Nb-13Ta-4.6Zr alloy[6] developed for biomedical applications, does not show Hooke's law, and that the α'' martensite phase has been recognized in the deformation microstructures of Ti-20Nb-10Ta-5Zr and Ti-25Nb-10Ta-5Zr alloys after tensile tests. The authors[1,3] showed that elastic behavior in a cold worked Ti-36Nb-2Ta-3Zr-0.3O alloy indicates a non-linearity in elasticity, with a gradient of the stress-strain curve in the elastic region continuously decreasing with increasing stress, furthermore, that is not accompanied by phase transformations, such as the stress-induced α''. The authors also found in the lower niobium content-containing alloy, Ti-32Nb-2Ta-3Zr-0.3O, that an obvious rearrangement of variants of α'' occurs, and the stress-strain curve can be explained by a reversible martensitic transformation. With regards to oxygen effects, Jablokov *et al.*[15] showed that oxygen acts as an interstitial strengthener in Ti-35.3Nb-5.1Ta-7.1Zr alloy,[16] which was the first developed Ti-Nb-Ta-Zr alloy for medical applications. The authors also showed in a previous paper[4] that as the oxygen content was increased, the generation of α'' and ω were suppressed and the yield strength was increased in Ti-36Nb-2Ta-3Zr-O alloys.

However, it is believed that a more detailed investigation on the relationship between the β phase stability and mechanical properties should be performed. In other words, there may be some room to improve the mechanical properties in the Ti-Nb-Ta-Zr-O system by further optimization of the alloy composition. In the present study, the effect of niobium (from 30 to 36%) and oxygen (from 0.3 to 0.5%) content on the β phase stability were first investigated using alloys whose compositions are around Ti-36Nb-2Ta-3Zr-0.3O. The effect of a brief aging treatment on the mechanical properties of the selected Ti-Nb-Ta-Zr-O alloy were also investigated in order to obtain a much higher strength with low Young's modulus.

2. Experimental Procedures

2.1 Basic concepts of controlling phase stability and microstructure

The authors have revealed that $(c_{11}\text{-}c_{12})$ takes a value close to zero around the composition of Ti-36Nb-2Ta-3Zr-0.3O alloy with an e/a value of around 4.24,[17] which just corresponds to the phase stability limit of β. When $(c_{11}\text{-}c_{12})$ approaches zero, the Young's modulus in $\langle 001 \rangle$ and the shear moduli along $\langle 011 \rangle$ on $\{011\}$ and along $\langle 111 \rangle$ on $\{011\}$, $\{112\}$ or $\{123\}$ exhibit very small values.[18] The above elastic anomaly in the alloy seems to contribute to a unique microstructure after plastic deformation, which is characterized by transgranular macroscopic crystal rotation, giant planar faults with local distorted area, and nano-order lattice

disturbances along specific crystallographic orientations.[19–22)]

Oxygen in the Ti-36Nb-2Zr-3Ta-O system is the most effective solid solution strengthening element, and also plays a very important role from a view point of the phase stability. Namely, a certain amount of oxygen suppresses the generation of α'' and ω, even though the β phase becomes unstable due to the very small (c_{11}-c_{12}) value.[4)] This is the reason why the Ti-36Nb-2Zr-3Ta-0.3O alloy has a low Young's modulus, which conventional titanium alloys could not achieve.[23)]

In order to gain a much higher strength without increasing the Young's modulus, it is a good way to optimize the phase stability and microstructure, while enhancing the solid solution through strengthening by oxygen. The basic concept adopted in the present study can be summarized as follows;

1. Optimizing the niobium content (which changes the phase stability) in the alloy with a rather high oxygen content.
2. Controlling the microstructure by aging treatment, changes the balance of high strength with low Young's modulus.

2.2 Manufacturing process of samples

The Ti-36Nb-2Ta-3Zr-0.3O alloy as a basic composition of the Ti-Nb-Ta-Zr-O system was used in this study. The niobium content was changed from 30 to 36%, and the oxygen content changed from 0.3 to 0.5% in order to examine the detailed relationship between the beta phase stability and mechanical properties.

Samples were prepared by a blended elemental method. Pure titanium powder and other powders for alloying, such as niobium, tantalum and zirconium, were blended at predetermined compositions in a rotation mill for 7.2 ks. The mixed powder was compacted into a cylindrical shape by cold isostatic pressing (CIP'ing) at a pressure of 392 MPa, sintered at 1573 K for 57.6 ks in a vacuum of 10^{-3} Pa, and cooled in a furnace to room temperature. The sintered billet was hot forged at 1423 K and subsequently formed into a round bar. The surface oxidized layer was peeled off, and the bar was then solution treated at 1323 K for 3.6 ks in an argon atmosphere, quenched in water, and then cold worked in a rotary swaging machine. Some of the alloys were further heat-treated at a temperature 623 K for less than 3.6 ks.

The oxygen content of the material was controlled by mixing in a titanium powder with high oxygen content (0.98% O). The niobium, tantalum, and zirconium contents of each sample were analyzed via Inductively Coupled Plasma-Atomic Emission Spectrometry and the oxygen content of that was determined with an oxygen/nitrogen analyzer. Table 1 shows the chemical alloy compositions of the experimental samples.

2.3 Evaluation of mechanical properties and microstructural analysis

Tensile tests were carried out on smooth cylindrical specimens (2 mm in diameter, 10 mm gauge length) at a strain rate of $5 \times 10^{-4}\ s^{-1}$ at room temperature. The tensile strain was measured using a strain gauge method to enable accurate evaluation of the Young's modulus and attainable elastic strain before plastic deformation. Two strain gauges were attached to the parallel portion of the specimen surface. The elastic limit strength was determined experimentally from the stress-strain curve. We defined the maximum strength in the stress-strain relation with no hysteresis as the elastic limit strength. The work hardening behavior was examined using the Vickers hardness test at a load of 49 N.

Table 1 Composition of the experimental alloys.

	Ti	Nb	Ta	Zr	O
Ti-32Nb-2Ta-3Zr-0.3O	bal	31.8	1.99	2.67	0.33
Ti-36Nb-2Ta-3Zr-0.3O	bal	35.7	1.97	2.66	0.31
Ti-30Nb-2Ta-3Zr-0.5O	bal	30.0	2.03	2.67	0.49
Ti-32Nb-2Ta-3Zr-0.5O	bal	31.9	2.10	2.68	0.49
Ti-33Nb-2Ta-3Zr-0.5O	bal	32.9	2.04	2.66	0.49
Ti-34Nb-2Ta-3Zr-0.5O	bal	33.9	2.11	2.70	0.49
Ti-36Nb-2Ta-3Zr-0.5O	bal	36.1	2.15	2.68	0.47

The microstructural characterizations were conducted using a combination of optical microscopy (OM), transmission electron microscopy (TEM), and X-ray diffraction (XRD). All specimens were prepared in the section vertical to the swaging direction. Polished specimens for OM were prepared by a conventional mechanical technique and were etched with an aqueous 10% HF + 10% HNO_3 solution. Specimens for XRD were prepared by chemical polishing. XRD was carried out using an X-ray diffractometer with Cu-Kα radiation at a scanning speed of 0.04 deg/s. The thin film for TEM analysis was cut into a small disk 0.5 mm thick, mechanically polished to 0.15 mm thick and electrolytically polished by the twin-jet method at 10 V. TEM observation was made at an acceleration voltage of 200 keV.

3. Results and Discussion

3.1 β phase stability depending on niobium and oxygen contents

Figure 1 shows the microstructures of the Ti-(32,36)Nb-2Ta-3Zr-0.3O alloys after water-quenching and the series of Ti-*X*Nb-2Ta-3Zr-0.5O alloys ($X = 30$ to 36%). The Ti-36Nb-2Ta-3Zr-0.3O alloy is composed of equiaxed β grains 50 to 100 μm in size. The acicular morphology of martensite is shown in the lower niobium content alloy, Ti-32Nb-2Ta-3Zr-0.3O. In the higher oxygen concentration alloy, Ti-32Nb-2Ta-3Zr-0.5O, the acicular morphology is not seen, and the structure morphology is almost the same as that of the Ti-36Nb-2Ta-3Zr-0.3O alloy. On the other hand, in the case of the alloy having an oxygen content of 0.5%, which subsequently lowers the niobium content to 30%, the acicular structure is seen in the microstructure. These results imply that the addition of oxygen shifts the martensite starting temperature, Ms, to a lower temperature.

In order to investigate the phase constitutions in the Ti-Nb-Ta-Zr-O system, XRD analysis was carried out at room temperature after a solution treatment at 1323 K for 3.6 ks. Figure 2 shows the XRD profiles of the Ti-(32,36)Nb-2Ta-3Zr-0.3O alloy, scanned from 30 to 80 degrees in diffraction angle (2θ), and the series of Ti-*X*Nb-2Ta-3Zr-0.5O alloys ($X = 30$ to 36%). In the case of alloys with 0.3% oxygen, the

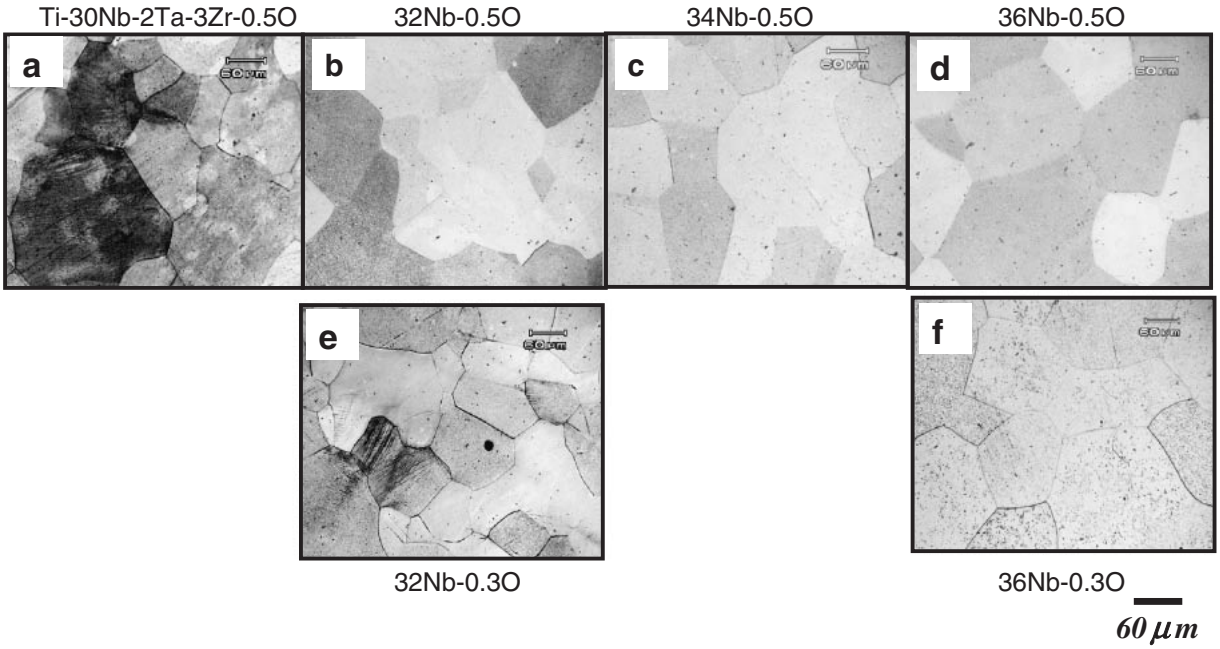

Fig. 1 Microstructures of the alloy specimens after solution treatment of (a), (b), (c) and (d) Ti-*X*Nb-2Ta-3Zr0.5O, and (e) and (f) Ti-*X*Nb-2Ta-3Zr0.3O. (a): $X = 30$. (b), (e): $X = 32$. (c): $X = 34$. (d), (f): $X = 36$.

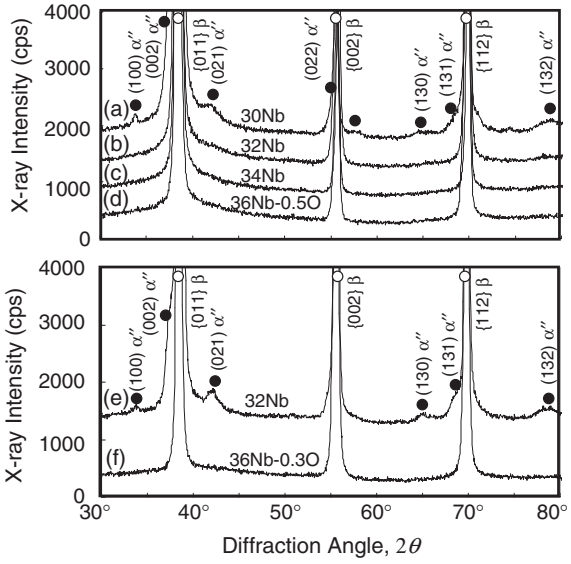

Fig. 2 X-ray diffraction profiles of the alloys after solution treatment of (a), (b), (c) and (d) Ti-*X*Nb-2Ta-3Zr0.5O, and (e) and (f) Ti-*X*Nb-2Ta-3Zr0.3O. (a): $X = 30$. (b), (e): $X = 32$. (c): $X = 34$. (d), (f): $X = 36$.

XRD profile of the Ti-36Nb-2Ta-3Zr-0.3O alloy exhibits only bcc peaks. On the other hand, the (002) and (021) peaks of orthorhombic α'' are apparently detected in the Ti-32Nb-2Ta-3Zr-0.3O alloy with strong bcc peaks. When the oxygen concentration was increased to 0.5%, it is clear that even the lower niobium containing alloy, Ti-32Nb-2Ta-3Zr-0.5O, is composed of a single β phase. The (002) and (021) orthorhombic peaks become clearly observable when the niobium content is lowered to 30%. Most commonly, under the Ti-O binary system, oxygen raises the β transus and promotes the formation of the α phase. Instead, however, the oxygen suppressed α'' in these alloys. This suggests that we can control the phase stability and enhance the solid solution strengthening by increasing the oxygen content.

Optical micrographs of the series of Ti-(32,36)Nb-2Ta-3Zr-0.3O alloys and the series of Ti-*X*Nb-2Ta-3Zr-0.5O alloys ($X = 30$ to 36%) after 90% cold working are shown in Fig. 3. The microstructure dramatically changes from that of before cold working, and the appearance of the microstructure depends on the niobium content. That is, the structures of the Ti-36Nb-2Ta-3Zr-0.3O, Ti-32Nb-2Ta-3Zr-0.5O, Ti-34Nb-2Ta-3Zr-0.5O and Ti-36Nb-2Ta-3Zr-0.5O alloys changed into a characteristic "marble-like" structure, composed of assemblies of fine filamentary structure. Although the microstructure of the alloys changed dramatically as seen in Fig. 3, the phase configuration did not change at all, even after heavy cold working. The XRD profiles after cold working did not show the presence of any peaks other than those of the β phase, as seen in Fig. 4. On the other hand, the stress-induced martensite microstructure is easily detected in the Ti-32Nb-2Ta-3Zr-0.3O and Ti-30Nb-2Ta-3Zr-0.5O alloys, although the peaks associated with the α'' diffraction are not as obvious as those in the solution-treated alloys.

It has been well known that the work hardening behavior is related to the plastic deformation behavior, which is strongly dependent on the β phase stability.[24] In this paper, the work hardening behavior was evaluated by calculating the work hardening ratio,[25] which is the ratio of the hardness after 90% cold working to that before cold working. Figure 5 shows the change in the work hardening ratio with niobium content. The plots for the alloys with 0.3% oxygen are previously reported in net. 25. The work hardening ratio of the alloys with a 0.3% oxygen content takes a minimum value at niobium contents of 36%. With decreasing niobium content, the phase configuration changes from the single β phase to the $\beta + \alpha''$ phase. Hanada *et al.*[26] reported that

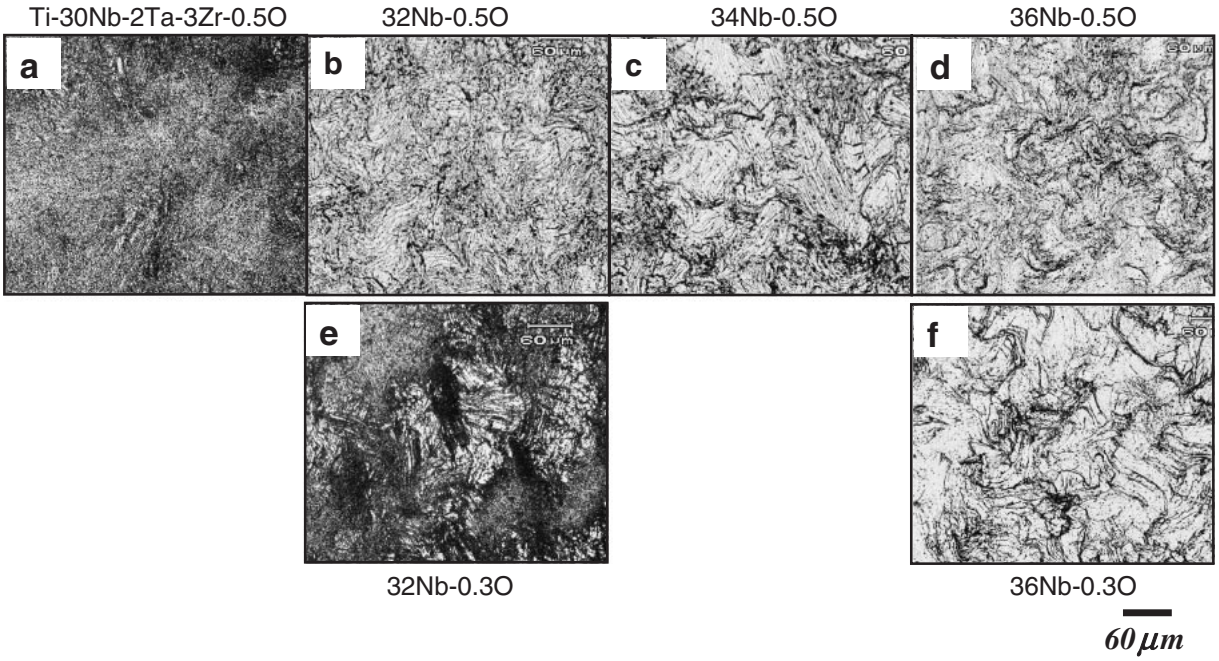

Fig. 3 Microstructures of the alloy specimens after cold working by 90% of (a), (b), (c) and (d) Ti-*X*Nb-2Ta-3Zr0.5O, and (e) and (f) Ti-*X*Nb-2Ta-3Zr0.3O. (a): $X = 30$. (b), (e): $X = 32$. (c): $X = 34$. (d), (f): $X = 36$.

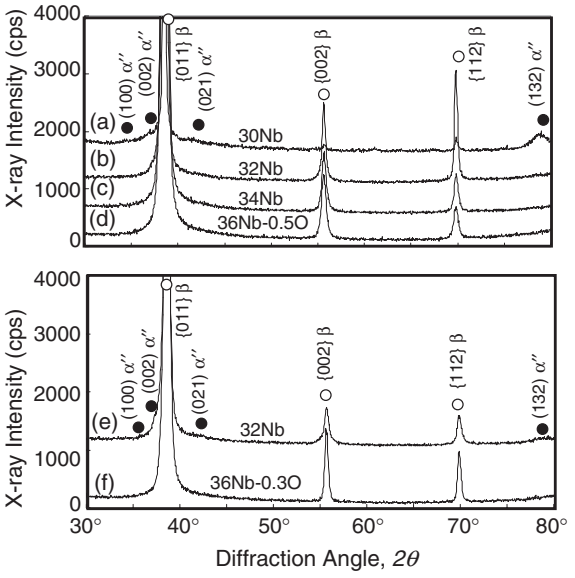

Fig. 4 X-ray diffraction profiles of the alloys after cold working by 90% of (a), (b), (c) and (d) Ti-*X*Nb-2Ta-3Zr0.5O, and (e) and (f) Ti-*X*Nb-2Ta-3Zr0.3O. (a): $X = 30$. (b), (e): $X = 32$. (c): $X = 34$. (d), (f): $X = 36$.

deformation at room temperature occurs by {332}⟨113⟩ twinning in the alloys whose Ms is near room temperature. The authors also reported that a high density dislocation configuration, composed of straight dislocations as well as tangled dislocations, was observed at the twin boundary.[27] From the observed results of the microstructure before and after cold working, it seems that the work hardening of the alloy with the lowest niobium content is relevant to the generation of the {332}⟨113⟩ twinning, which was observed in the previous study.[27] Consequently, several dislocations occurred in the stress-induced martensite microstructure by mechanical twinning during cold working.

The minimum value of that in the alloys with an oxygen content of 0.5% shifts to around that of the alloy with a 33% niobium content. The minimum value of the work hardening ratio of both oxygen content alloys is as low as 5%, which means that these alloys are difficult to work-harden even after a severe cold working process with a reduction in area of 90%. Of course, the hardness itself increases by the addition of oxygen, but it is inferred from these results that dislocation-free plastic deformation due to an elastic anomaly, which was seen in the Ti-36Nb-2Ta-3Zr-0.3O alloy,[20] also operates as a dominant mechanism in the lower niobium alloy with higher oxygen content.

3.2 Effect of the niobium content on mechanical properties of the cold worked Ti-Nb-Ta-Zr-O alloys with 0.5% oxygen content

Figure 6 shows the tensile strength, elongation and Young's modulus of the cold worked Ti-(30-36)Nb-2Ta-3Zr-0.5O alloys at room temperature. The tensile strength increased with decreasing niobium content, while the elongation decreased with decreasing niobium content; the elongation of the Ti-30Nb-2Ta-3Zr-0.5O alloy was lowered to about 7%. In addition, the change in Young's modulus with niobium content indicates an interesting tendency. It takes a minimum value of around 33% niobium content, which almost corresponds to the niobium content showing the phase stability limit of β (Fig. 3, 4) and a minimum work hardening ratio (Fig. 5). This tendency is in good agreement with the results reported by Matsumoto *et al.*,[28] who have also shown that the Young's modulus exhibits a minimum when Ms is close to room temperature. It is inferred from the results in Figs. 3–6 that the critical niobium content required for stable β, in which the dislocation-free plastic deformation mechanism operates due to the elastic anomaly, shifts to a lower niobium content by the addition of oxygen.

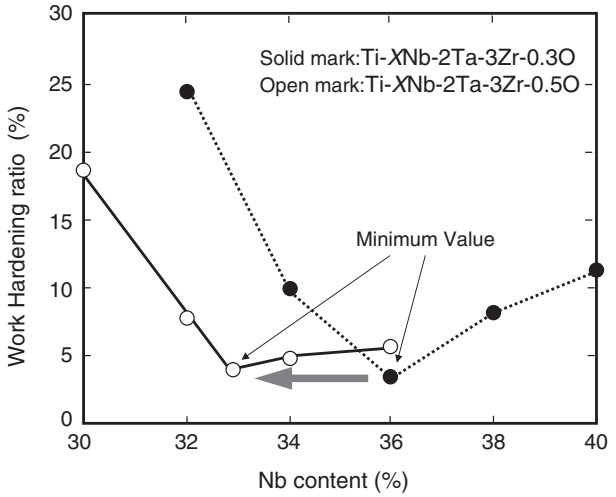

Fig. 5 Work hardening ratio vs. Nb content of Ti-*X*Nb-2Ta-3Zr0.3O and Ti-*X*Nb-2Ta-3Zr0.5O.

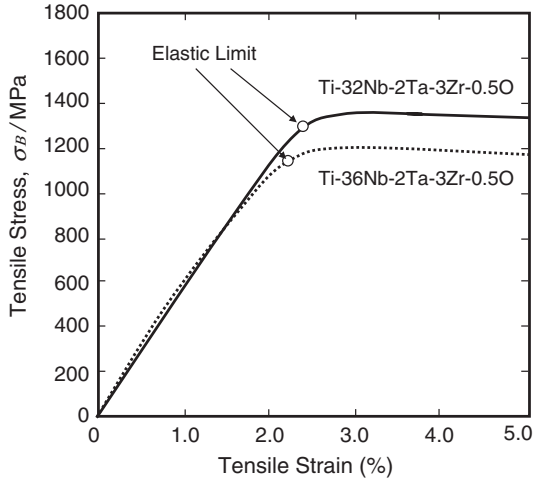

Fig. 7 Tensile stress-strain curves of the cold worked Ti-36Nb-2Ta-3Zr-0.3O and Ti-32Nb-2Ta-3Zr-0.5O alloys.

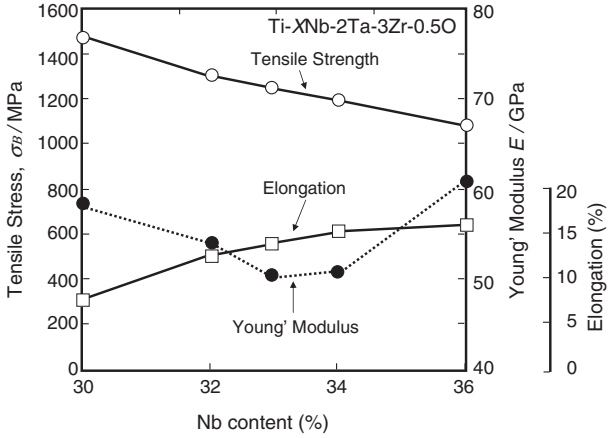

Fig. 6 Changes in tensile strength, Young's modulus and elongation with Nb content of Ti-*X*Nb-2Ta-3Zr-0.5O.

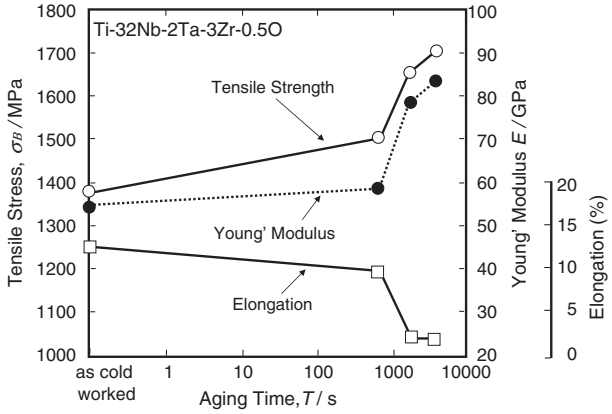

Fig. 8 Mechanical properties after aging treatment of the cold worked Ti-32Nb-2Ta-3Zr-0.5O alloy as a function of aging time. Aging temperature is 623 K.

By analyzing the details of the stress-strain curves of the cold worked samples, the elastic deformation behavior of the Ti-36Nb-2Ta-3Zr-0.3O alloy indicates non-linearity in elasticity. By the addition of oxygen, the elastic deformation behavior is reported to change in linearity and show a higher rigidity than that of the Ti-36Nb-2Ta-3Zr-0.3O alloy.[4] This phenomenon can be understood if the oxygen atoms play a role in suppressing the lattice movement during the elastic deformation. As seen in Fig. 7, it was found that a slight modification in niobium content in the alloy with 0.5% oxygen shows a good combination of Young's modulus and yield strength. The Ti-32Nb-2Ta-3Zr-0.5O alloy indicates a Young's modulus of 55 GPa with linearity in elasticity; a tensile strength of 1370 MPa and a tensile elongation of 12% (see also Fig. 6).

3.3 Effect of a brief aging treatment on Young's modulus and tensile strength

An aging treatment is a very effective way for obtaining a high strength titanium alloy through precipitation hardening.[29] This process however, often raises the Young's modulus as well as the tensile strength. In the case of

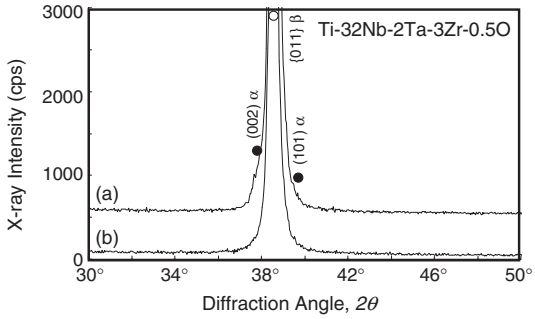

Fig. 9 X-ray diffraction profiles after aging treatment of the cold worked Ti-32Nb-2Ta-3Zr-0.5O alloy. (a): at 623 K for 3.6 ks. (b) at 623 K for 600 s.

metastable titanium alloys, the Young's modulus is strongly related to the isothermal ω and precipitation of the α phase in the β phase after heat treatment.[30] Therefore, the most important thing is how to control the precipitation behavior of ω and α, in order to obtain the Ti-Nb-Ta-Zr-O alloy having low Young's modulus with high strength. With these points in mind, we will next take a look at the aging behavior of the

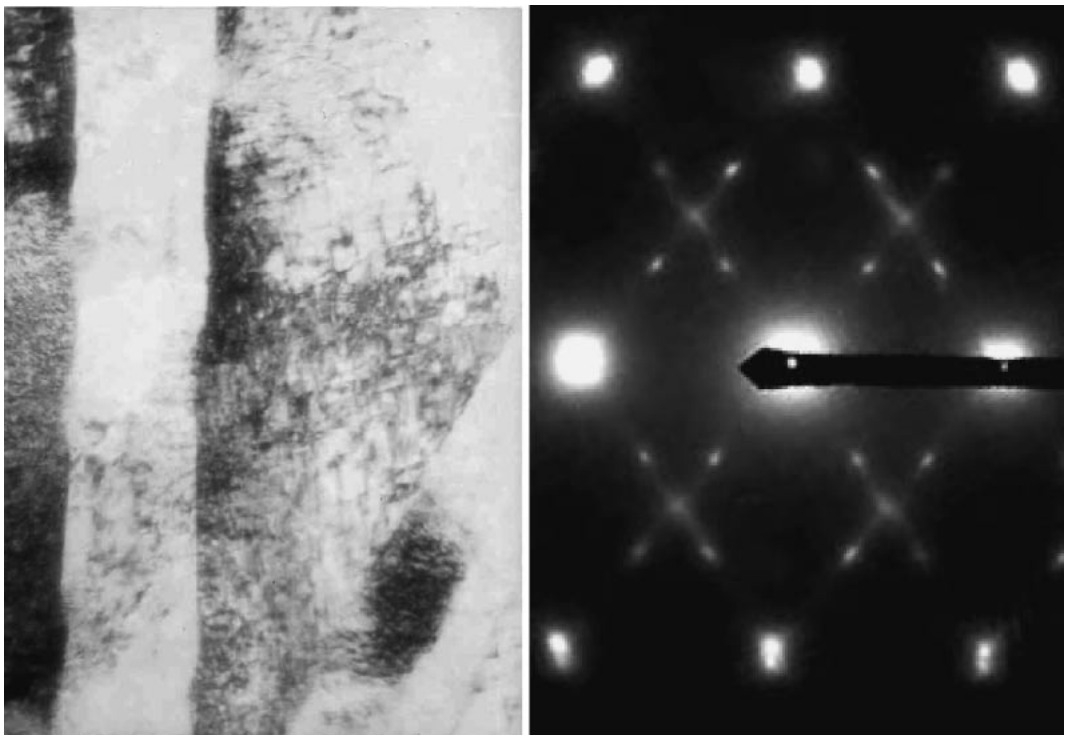

Fig. 10 TEM microstructures of the Ti-32Nb-2Ta-3Zr-0.5O alloy cold worked and aged 623 K of 600 s.

cold worked Ti-32Nb-2Ta-3Zr-0.5O alloy. Figure 8 shows changes in the tensile strength, elongation and Young's modulus of the cold worked Ti-32Nb-2Ta-3Zr-0.5O alloy with aging at 623 K. The tensile strength gradually increased with increasing aging time up to 600 s, and then suddenly increased reaching 1700 MPa at 3.6 ks. Here, the observed changes in Young's modulus and elongation have the same tendency as the abrupt change, being approximately constant up to 600 s, and then drastically changed; the Young's modulus increased to a higher value of 83 GPa, while the elongation decreased to a lower value of 1.5% at 3.6 ks. It is considered that the change in these properties after aging for 3.6 ks is mainly attributed to precipitation of the α phase, as seen in Fig. 9. On the other hand, during aging times less than 600 s, no reflections from the ω and α phases were detected by XRD. However, the tensile strength is seen to increase from 1370 MPa to 1500 MPa with increasing aging time. The phenomenon of phase transformation during the relatively low temperature aging treatment of the metastable β titanium alloys has been reported by many researchers. For example, Ikeda *et al.*[31] reported that by using the detailed electrical resistivity measuring method, the isothermal ω precipitation from the metastable β phase occurred by way of some clustering process in the β phase, which continuously occurred at an aging temperature 573 K, although no reflections from the ω and α phases were detected by XRD. Another paper reported[32] that the isothermal ω dense distribution of fine particles, plays a role as a precursor to the α phase, because the hexagonal-close-packed structure of the α phase cannot be readily nucleated in the beta phase. Hickman[33] reported that the regimes of occurrence of the isothermal ω is up to 723 K in the case of the Ti-10Nb and Ti-30Nb (at%) systems.

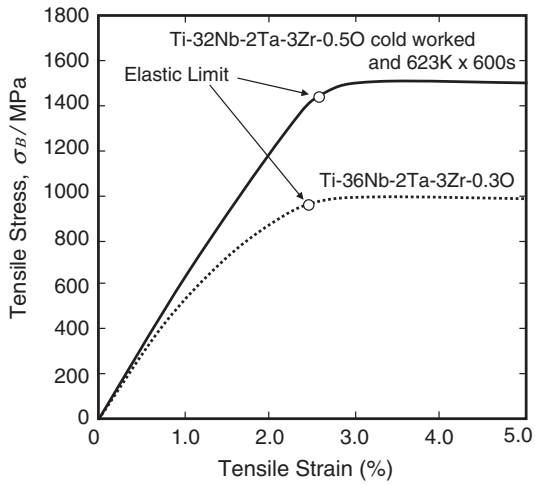

Fig. 11 Tensile stress-strain curves of the cold worked Ti-36Nb-2Ta-3Zr-0.3O and Ti-32Nb-2Ta-3Zr-0.5O alloys cold worked and aged at 623 K of 600 s.

Figure 10 shows an example of TEM observation of the Ti-32Nb-2Ta-3Zr-0.5O alloy cold worked and aged at 623 K for 600 s. As is clear from Fig. 10, the weak ω reflections are shown in the electron diffraction pattern of the aged Ti-32Nb-2Ta-3Zr-0.5O alloy. It is inferred from the TEM observation results that the improvement of strength by the aging treatment up to 600 s without increasing Young's modulus, is referred to as a very fine isothermal ω, which is impossible to detect by XRD.

Figure 11 shows the elastic deformation behavior of the cold worked Ti-36Nb-2Ta-3Zr-0.3O alloy and the Ti-32Nb-2Ta-3Zr-0.5O alloy cold worked and aged at 623 K for 600 s.

The initial Young's modulus and attained elastic strain of the Ti-32Nb-2Ta-3Zr-0.5O alloy are almost the same as those of the Ti-36Nb-2Ta-3Zr-0.3O alloy, which are about 58 GPa and 2.5%, respectively. On the other hand, the elastic deformation behavior of the alloys is completely different; the Ti-32Nb-2Ta-3Zr-0.5O alloy has a linear stress-strain relationship in the elastic range. Furthermore, the most important point to emphasize is the fact that the tensile strength is approximately 1.5 times as high as that of the Ti-36Nb-2Ta-3Zr-0.3O alloy with almost no change in Young's modulus.

Detailed quantitative evaluations of the elastic and plastic behavior are subjects of future study; however, the present study revealed that it is possible to control the phase stability limit of β with enhancement of the solid solution strengthening by oxygen. The brief aging treatment under such kind of β phase stability has been also found to be the most effective microstructure control method for achieving high strength with low Young's modulus in Ti-Nb-Ta-Zr-O alloys by the authors.

4. Summary

The effects of niobium and oxygen content on the mechanical properties, β phase stability and elastic deformation behavior in Ti-Nb-Ta-Zr-O alloys were investigated in this study. The following results were obtained.

(1) The addition of oxygen shifts the phase stability limit of β to a lower niobium content, and the phase stability can be controlled with enhancing solid solution hardening by oxygen.

(2) The elastic deformation behavior of the cold worked Ti-32Nb-2Ta-3Zr-0.5O alloy indicated linearity in elasticity with increasing tensile strength, compared with that of the Ti-36Nb-2Ta-3Zr-0.3O alloy. The Ti-32Nb-2Ta-3Zr-0.5O alloy had a low Young's modulus of 55 GPa, a high tensile strength of 1370 MPa and a tensile elongation of 12%.

(3) After subsequent aging at 623 K for 600 s, the Ti-32Nb-2Ta-3Zr-0.5O alloy indicated a low Young's modulus of 58 GPa, a higher tensile strength of 1500 MPa, and a tensile elongation of 10%. This tensile strength value is approximately 1.5 times as high as that of Ti-36Nb-2Ta-3Zr-0.3O with almost no change in Young's modulus.

REFERENCES

1) T. Furuta, K. Nishino, J. H. Hwang, A. Yamada, K. Ito, S. Osawa, S. Kuramoto, N. Suzuki, R. Chen and T. Saito: Ti-2003 Science and Technology, ed. by G. Lütjering and J. Albrecht, (WILEY-VCH, Weinheim, 2004) pp. 1519–1526.
2) T. Furuta, S. Kuramoto, J. H. Hwang, K. Itoh and T. Saito: Materia Japan **43** (2004) 154–156.
3) T. Furuta, S. Kuramoto, J. H. Hwang, K. Nishino and T. Saito: Mater. Trans. **46** (2005) 3001–3007.
4) T. Furuta, S. Kuramoto, R. Chen, J. H. Hwang, K. Nishino and T. Saito: J. Japan Inst. Metals. **70** (2006) 579–585.
5) S. Kuramoto, T. Furuta, J. H. Hwang, K. Nishino and T. Saito: J. Japan Inst. Metals. **69** (2005) 953–961.
6) M. Niinomi: Mater. Sci. Eng., A **243** (1998) 231–236.
7) D. Kuroda, M. Niinomi, K. Fukui, A. Suzuki and J. Hasegawa: Tetsu–to-Hagane **86** (2000) 610–616.
8) T. Akahori, M. Niinomi, T. Maekawa, K. Fukui and A. Suzuki: J. Japan Inst. Metals. **66** (2002) 715–722.
9) M. Niinomi, T. Akahori, T. Yabunaka, K. Fukui and A. Suzuki: Tetsu–to-Hagane **88** (2002) 553–560.
10) M. Niinomi, T. Akahori, S. Nakamura, K. Fukui and A. Suzuki: Tetsu–to-Hagane **88** (2002) 567–574.
11) M. Niinomi: Biomaterials **24** (2003) 2673–2683.
12) M. Long and H. J. Rack: Biomaterials **19** (1998) 1621–1639.
13) D. Kuroda, M. Niinomi, M. Morinaga, Y. Kato and Y. Yashiro: Mater. Sci. Eng., A **243** (1998) 244–249.
14) N. Sakaguchi, M. Niinomi and T. Akahori: Mater. Trans. **45** (2004) 1113–1119.
15) V. R. Jablokov, N. G. D. Murray, H. J. Rach and H. L. Freese: J. ASTM International **2** (2005) 1–12.
16) T. Ahmed, M. Long, J. Silvestri, C. Ruiz and H. J. Rack: *Titanium '95 Science and Technology*, ed. by P. A. Blankinsop, W. J. Evans, F. H. Flower, (The Material Society, London, 1996) pp. 1760–1767.
17) H. Ikehata, N. Nagasako, T. Furuta, A. Fukumoto, K. Miwa and T. Saito: Phys. Rev. B **70** (2004) 174113-1-174113-8.
18) C. R. Krenn, D. Roundry, J. W. Morris Jr. and M. L. Cohen: Mater. Sci. Eng., A **319–321** (2001) 111–114.
19) T. Saito *et al.*: Science **300** (2003) 464–467.
20) S. Kuramoto, T. Furuta, J. H. Hwang, R. Chen, K. Nishino and T. Saito: Materia Japan **43** (2004) 840–844.
21) S. Kuramoto, T. Furuta, J. H. Hwang, K. Nishino and T. Saito: Metall. Mater. Trans. A **37A** (2006) 657–662.
22) M. Y. Gutkin, T. Ishizaki, S. Kuramoto and I. A. Ovid'ko: Acta Mater. **54** (2006) 2489–2499.
23) E. S. Fisher and D. Dever: Acta Metall. **18** (1970) 265–269.
24) S. Hanada and O. Izumi: Metall. Trans. A **18A** (1987) 265–271.
25) J. H. Hwang, S. Kuramoto, T. Furuta, K. Nishino and T. Saito: J. Mater. Eng. Perf. **14** (2005) 747–754.
26) S. Hanada and O. Izumi: Metall. Trans. A **17A** (1986) 1409–1420.
27) S. Hanada, M. Ozeki and O. Izumi: Metall. Trans. A **16A** (1985) 789–795.
28) H. Matsumoto, S. Watanabe and S. Hanada: Mater. Trans. **46** (2005) 1070–1078.
29) R. Boyer, G. Welsch and E. W. Collings: *Material Properties Handbook, Titanium Alloy*, (ASM International, Ohio, 1994) pp. 100–106.
30) R. Boyer, G. Welsch and E. W. Collings: *Material Properties Handbook, Titanium Alloy*, (ASM International, Ohio, 1994) pp. 94–100.
31) M. Ikeda, S. Komatsu, I. Sowa and M. Niiinomi: Metall. Mater. Trans. A **33A** (2002) 487–493.
32) R. Boyer, G. Welsch and E. W. Collings: *Material Properties Handbook, Titanium Alloy*, (ASM International, Ohio, 1994) pp. 1051–1060.
33) B. S. Hickman: J. Mater. Sci. **4** (1969) 554–563.